Online ISSN: 2981-0396 Print ISSN: 2981-0388

International Journal of Iron & Steel Society of Iran

Journal Homepage: https://journal.issiran.com/

Research Article

Effect of Carbon Addition on the Corrosion Properties of FeCoCrMnNi High Entropy Alloy

A. Pourbesharati [1], R. Amini Najafabadi *[2], T. Isfahani [3]

Materials Engineering Group, Golpayegan College of Engineering, Isfahan University of Technology, Golpayegan, Iran

ARTICLE INFO

Keywords:

Carbon Addition, Corrosion Properties, FeCoCrMnNi, High Entropy Alloy.

Article history:

Received 23 April 2024
Received in revised form 11 May 2024
Accepted 06 August 2024

ABSTRACT

Alloying is a technique that has long been used to provide desirable properties in materials. It mainly involves the addition of relatively small amounts of secondary elements to a primary element. Recently, a new alloying strategy that involves the combination of multiple principal elements in high concentrations to create new materials called high-entropy alloys has been investigated by several researchers. In this paper, the thermodynamic calculations and phase formation rules for the formation of FeCoCrMnNi high entropy alloy are discussed. The FeCoCrMnNi and $FeCoCrMnNiC_{0.2}$, high entropy alloys were cast using a vacuum arc melting furnace. It was shown that both of the high entropy alloys formed a single FCC solid solution phase without any other impurities or phases. The whole pattern Rietveld refinement analysis showed that the addition of carbon to the FeCoCrMnNi high entropy alloy decreased the crystallite size. Moreover, the Tafel corrosion test results indicated that the corrosion resistance of the FeCoCrMnNi high entropy alloy increased 185 times with the addition of carbon.

1. Introduction

In the recent years the newly developed high-entropy alloys (HEAs) introduced by Yeh [1] and Cantor [2] have attracted the attention of many researchers and industries [3-5]. In contrast to traditional alloys, which have one or two main components, high-entropy alloys have at least five main elements with atomic concentrations between 5% and 35% [3, 4, 6, 7]. The high entropy alloys are mainly designed to obtain solid-solutions rather than forming complex phases. It has been shown by many researchers that the equiatomic and non-equiatomic HEAs provide great potentials of engineering application due to their high oxidation, corrosion, wear resistance, high ductility, and strength [6-11]. However, the properties of high entropy alloys are affected by their chemical composition. The chemical composition determines the type of the formed solid solution phase(s) [12]. For example, the FCC solid-solution phases are most probably formed when elements such as Ni, Mn and Cu are used whereas the use of W, Ti, V and Al form BCC solid solution phases. The addition of another element to an HEA or the change in the amount of an element present in the HEA effects on the physical properties and structural formation of the alloy. These changes are due to the different atomic radius and atomic percent of the atoms present in the alloy resulting in different amounts of high mixing

*Corresponding author
Email: r.amini@iut.ac.ir
Address: Materials Engineering Group, Golpayegan College of Engineering, Isfahan University of Technology, Golpayegan, Iran
1. M.S., Candidate, 2. Associate Professor, 3. Assistant Professor

DOI: http://10.22034/IJISSI.2024.2027144.1288
Published by ISSI (Iron & Steel Society of Iran)

entropy (ΔS_{mix}) and mixing enthalpy (ΔH_{mix}) which are the critical decisive factors for the formation of the solid-solution structures. One of the important high entropy alloys is Cantor's alloy. Cantor arc melted down a separate ingot of equimolar Co-Cr-Fe-Mn-Ni referred to as the Cantor alloy or Cantor's alloy[13-15].

In this study FeCoCrMnNi and $FeCoCrMnNiC_{0.2}$ high entropy alloys were fabricated by vacuum arc-melt casting and the effect of carbon addition on the structural and corrosion properties were investigated.

2. Materials and methods

Appropriate amounts of pure (99.95%) Fe, Co, Cr, Mn, Ni and carbon source were used as raw material to produce the FeCoCrMnNi and $FeCoCrMnNiC_{0.2}$ high entropy alloys according to Table1. The raw materials used were in high purity. The alloys were melted in a high vacuum arc melting furnace. In order to obtain chemical homogeneity, the melting was repeated three times. The sample was flipped over after each melting and melted again. Samples for crystal structure and corrosion investigation were taken out from the alloy button by the aid of an EDM wire cutting machine. The phase analysis was performed using an ASENWARE (AW-XDM) x-ray diffraction machine with CuKα radiation (λ= 1.542 Å) in the 2Θ scan range of 20°-90°. The crystallite size was determined by the use of the whole pattern Rietveld analysis applied by the use of MAUD software [16]. Thermodynamic analysis was carried out using the extended Miedema model [17]. The corrosion tests were applied using an OrgaLys potentiostat machine. The 3.5% NaCl solution was used to perform the tests. The corrosion data were revealed from the Tafel polarization curves.

3. Results and Discussion

3.1. Investigation on the criteria of the HEA formation

There is limited thermodynamic data on HEAs which is due to the lack of quaternary and higher phase diagrams. Therefore, the prediction of phase formation by the use of known properties such as melting point, entropy, and enthalpy of mixing is essential. In this section, thermodynamic calculations are done to obtain more information on the phase(s) formed during the casting process as below:

To obtain the average melting point of an n-component alloy (T_m), Eq.(1) can be used:

$$T_m = \sum_{i=1}^{n} C_i \, (T_m)_i \qquad \text{Eq.(1)}$$

whereas C_i is the atomic percent of the i-th component and $(T_m)_i$ is the melting point of the i-th component.

The valence electron concentration (VEC) and electronegativity difference ($\Delta\chi$) are calculated from Eqs. (2 and 3), respectively. Whereas χ_i and $\overline{\chi}$ are the Pauling electronegativity of the i-th component and average electronegativity difference Eq.(4), respectively.

$$VEC = \sum_{i=1}^{n} C_i \, (VEC)_i \qquad \text{Eq.(2)}$$

$$\Delta x = \sqrt{\sum_{i=1}^{n} C_i \, (\chi_i - \overline{\chi})^2} \qquad \text{Eq.(3)}$$

$$\overline{\chi} = \sum_{i=1}^{n} C_i \chi_i \qquad \text{Eq.(4)}$$

The atomic size difference (δ) is determined by Eq.(5):

$$\delta = 100 \sqrt{\sum_{i=1}^{n} C_i \, (1 - \frac{ri}{\bar{r}})^2} \qquad \text{Eq.(5)}$$

whereas $\bar{r}$ can be calculated from the atomic radius of the components (Å) as Eq.(6).

$$\bar{r} = \sum_{i=1}^{n} C_i \, r_i \qquad \text{Eq.(6)}$$

The ΔS_{mix} and ΔH_{mix} are the mixing entropy change and mixing enthalpy and are obtained by Eqs. (7 and 8) while R (the constant gas is considered to be 8.314 $J/mol^{-1}K^{-1}$, Ω_{ij} is the regular melt interaction parameter between the i-th and j-th element Eq.(9) and C_i and C_j are the atomic percentage of the i-th and j-th component change of the binary liquid AB alloy. The (ΔH_{mix}^{AB} (J/mol^{-1})) is calculated by the Miedema's model.

$$\Delta S_{mix} = -R \sum_{i=1}^{n} C_i \ln C_i \qquad \text{Eq.(7)}$$

$$\Delta H_{mix} = \sum_{i=1, i\neq j}^{n} \Omega_{ij} \, C_i C_j \qquad \text{Eq.(8)}$$

$$\Omega_{ij} = 4 \, \Delta H_{mix}^{AB} \qquad \text{Eq.(9)}$$

Table 1. Weight percent of the raw materials used for the casting of the high entropy alloys.

Alloy	Fe	Co	Cr	Mn	Ni	C
FeCoCrMnNi	19.92	21.02	18.54	19.59	20.93	-
$FeCoCrMnNiC_{0.2}$	19.75	20.84	18.39	19.43	20.75	0.85

The elements present in the HEAs and their amounts have a significant influence on the microstructure and properties. It has been shown that the high mixing entropy of HEAs is the main reason for avoiding the formation of intermetallic compounds. Whereas the formation of solid solution(s) is due to the negative values of the ΔH_{mix}, ΔS_{mix}, δ and also sluggish diffusion. The ΔH_{mix} and δ have a nearly zero value for the formation of a solid solution. The phase formation in the HEAs is determined by the competition between ΔS_{mix}, ΔH_{mix}, and δ as below:

$$-10 \leq \Delta H_{mix} \leq -5 \text{ KJ.mol}^{-1} , \delta \leq 4\% ,$$
$$\Delta S_{mix} \geq 13.38 \text{ J.mol}^{-1}.\text{k}^{-1}$$

The Ω parameter, which is dependent on the ΔS_{mix} and ΔH_{mix} is as Eq.(10):

$$\Omega = \frac{T_m \Delta S_{mix}}{\Delta H_{mix}} \quad \text{Eq.(10)}$$

Whereas T_m is the average melting point of the alloy. The δ and Ω parameters should be as below to have obtained a solid solution(Eq.(11)):

$$\delta \leq 6.6\% , \Omega \geq 1.1 \quad \text{Eq.(11)}$$

To determine the structure of the solid solution and the phase stability, the VEC should be considered as the following criteria (Eq.(12)):

$$(\text{BCC}) 6.87 \leq \text{VEC} = \sum_{i=1}^{n} C_i \text{ (VEC)} < 8 (\text{FCC}) \quad \text{Eq.(12)}$$

3.2. Thermodynamic calculations

The ΔH_{mix}, ΔS_{mix}, δ, VEC, T_m, and Δx parameters are calculated for the FeCoCrMnNi HEA as presented in Table 2.

In Table 3. the amount of ΔH_{mix}^{AB} are calculated using the Mediema model for binary compounds in the FeCoCrMnNi HEA system.

According to Eq.(12), VEC values lower or equal to 6.87 stabilize BCC structure while values higher than 8 stabilize the FCC structure. However, for amounts between 6.87 and 8 both BCC and FCC structure are stabilized. Therefore, we expect FCC structure to be obtained.

Furthermore, the calculated values for ΔH_{mix}, δ and ΔS_{mix} as presented in Table 2. confirm the formation of solid solution.

Table 2. Calculated amounts of ΔH_{mix}, ΔS_{mix}, δ, VEC, T_m , Δx parameters.

Δx	**T_m (k)**	**VEC**	**(Å) δ**	**ΔS_{mix} ($j.mol^{-1}k^{-1}$)**	**ΔH_{mix} (j/mol)**	**ΔG_{mix} (Kj/mol)**
1.417129	1800.929	8.000055	1.6291	13.38087	-5160.74	-8.15024

Table 3. The calculated amounts of ΔH_{mix}^{AB} (J/mol-k) obtained by using the Mediema model [18].

Element	**Co**	**Cr**	**Fe**	**Ni**	**Mn**
Co	–	-16	-4	0	-20
Cr		–	-4	-28	8
Fe			–	-8	0
Ni				–	-32
Mn					–

Investigation on the binary phase diagrams indicates that a number of binary compounds could probably be formed and therefore they need to be investigated in detail. The ΔG_{mix} of the binary compounds is calculated and presented in Table 4. As can be seen these amounts have higher values compared to the ΔG_{mix} of the FeCoCrMnNi HEA confirming that the solid solution of the FeCoCrMnNi HEA will be formed instead of the binary intermetallic compounds presented in Table 4.

3.3. XRD studies

The XRD patterns of the FeCoCrMnNi and FeCoCrMnNi$C_{0.2}$ HEAs are presented in Fig. 1. As can be seen both patterns are similar and show an FCC structure indicating that the elements have formed a solid solution without any impurities and other phases such as intermetallic phases. However, the peak intensities of the FeCoCrMnNi$C_{0.2}$ HEA alloy is slightly lower than the FeCoCrMnNi HEA which indicates a lower crystallinity is obtained with the addition of carbon in the FCC solid solution phase. The whole pattern Rietveld refinement analysis was applied to the XRD patterns to obtain the crystallite size of the samples. The crystallite size was measured to be 369 and 308 nm for the FeCoCrMnNi and FeCoCrMnNi$C_{0.2}$ HEAs, respectively (Table 5). This indicates that the carbon addition has reduced the crystallite size of the single FCC solid solution phase. As expected with the addition of carbon to the lattice the lattice expands resulting increasing of the lattice parameter and reduction of the crystallite size. It is also well known that in steels, the increase of carbon in the form of solid solution increases the dislocation density and refines the crystallite size. Therefore, in addition to the solid solution strengthening owing to supersaturated C in solid solution the dislocation strengthening and grain refinement strengthening increase with the increase in the C content [19].

3.4. Corrosion Behavior of the FeCoCrMnNi and FeCoCrMnNi$C_{0.2}$ HEAs

In Figs. 2 (a) and (b), the Tafel polarization curve of the FeCoCrMnNi and FeCoCrMnNi$C_{0.2}$ high entropy alloys are presented, respectively. The corrosion parameters extracted from the curves are shown in Table 6. It is well known that factors such as the corrosive media and materials composition affect the corrosion resistance of materials. In this research the 3.5% NaCl solution as a corrosive environment is the same for the different samples, as can be seen, the corrosion resistance and corrosion current density of the samples are different which is due to the different compositions of the high entropy alloy samples. As can be seen, the addition of carbon improves the corrosion resistance, having a lower amount of corrosion current density and corrosion rate to be 0.0044 $\mu A/cm^2$ and 0.024 µm/Y, respectively. In other words, the corrosion rate of the FeCoCrMnNi alloy (4.42) is 185 times higher than the FeCoCrMnNi$C_{0.2}$ alloy.

As mentioned according to the presented results of Table 2. the corrosion resistance increases for the FeCoCrMnNi$C_{0.2}$ HEA containing carbon. This is due to the reason that probably the addition of carbon provides the necessary conditions for the formation of a protective layer against corrosion.

Table 4. The ΔG_{mix} of the intermetallic compounds that can possibly be formed.

	Fe_3Ni	**$FeNi_3$**	**FeNi**	**Ni_2Cr**
ΔG_{mix} (Kj/mol)	-1.16	-1.16	-1.55	-5.9

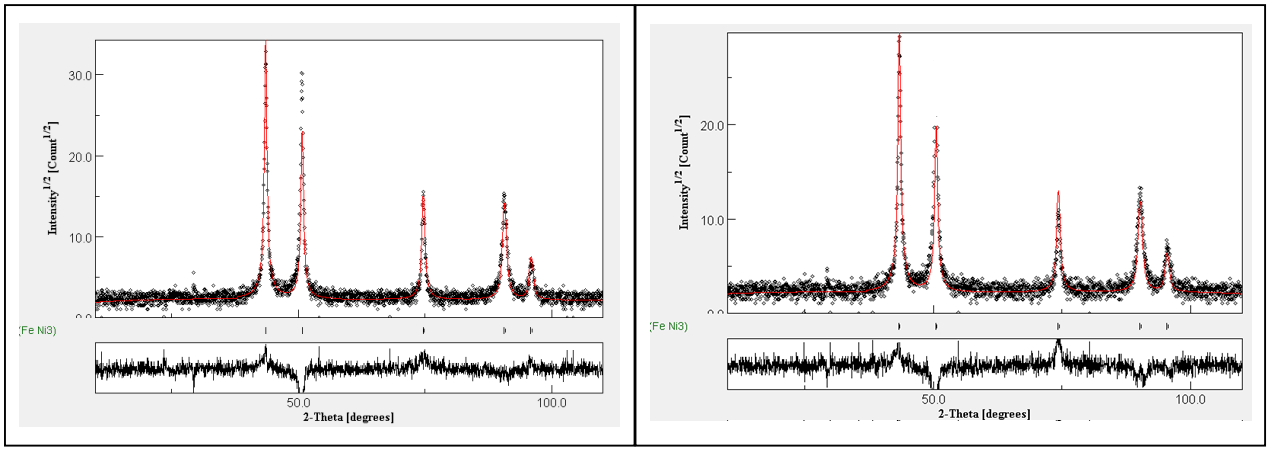

Fig. 1. The whole pattern Rietveld refinement of the: (a) FeCoCrMnNi and (b) and FeCoCrMnNi$C_{0.2}$ high entropy alloys.

Table 5. The results of the whole pattern Rietveld refinement analysis for the FeCoCrMnNi and $FeCoCrMnNiC_{0.2}$ high entropy alloys.

Sample	a (Å)	Crystallite size (nm)
FeCoCrMnNi	3.590	368.77
$FeCoCrMnNiC_{0.2}$	3.610	307.59

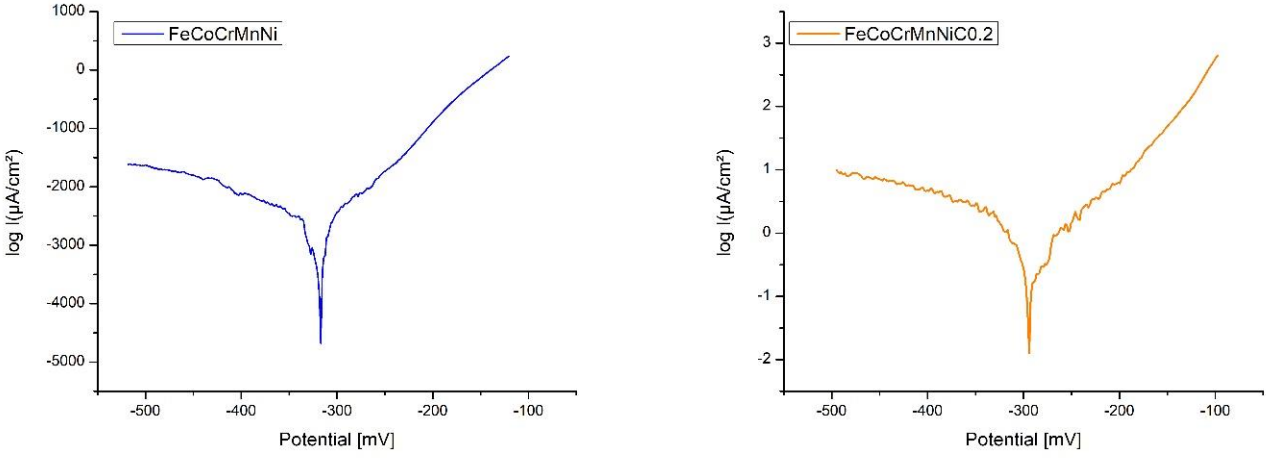

Fig. 2. Tafel polarization corrosion plots of (a) FeCoCrMnNi and (b) $FeCoCrMnNiC_{0.2}$ high entropy alloys.

Table 6. The results of the Tafel polarization corrosion test applied on the FeCoCrMnNi and $FeCoCrMnNiC_{0.2}$ high entropy alloys.

Samples	β_a(mV)	$-\beta_c$(mV)	E_{corr} (i=0) (mV)	i_{corr} (μA/cm²)	R_p (kOhm.cm²)	CR (μm/Y)
FeCoCrMnNi	55	104.2	-319.8	0. 8	7.23	4.42
$FeCoCrMnNiC_{0.2}$	38.3	53.3	-296.4	0.0044	178.83	0.024

4. Conclusions

In this study, FeCoCrMnNi and $FeCoCrMnNiC_{0.2}$ high entropy alloys were prepared from vacuum arc melt casting. The thermodynamic calculations and XRD patterns revealed that both of the alloys had a single FCC solid solution phase. The crystallite sizes were determined by the whole pattern Rietveld refinement method which indicated that the addition of carbon results in the increase of the lattice parameter and decrease in the crystallite size from 369 to 308 nm. Furthermore, the Tafel corrosion test showed that the corrosion resistance of $FeCoCrMnNiC_{0.2}$ high entropy alloy was 185 times more than the FeCoCrMnNi.

References

[1] Yeh J.W, C.S.L.S, Gan j.Y, Chin T.S, Shun T.I, Nanostructured High-Entropy Alloys with Multiple Principal Elements: Novel Alloy Design Concepts and Outcomes, Advanced Engineering Materials. 2004; 6: 299-303.
[2] Cantor B, Chang I.T.H, K.P, Vincent A.J.B, Microstructural development in equiatomic multicomponent alloys, JournalMaterials science and engineering a-Structural materials properties microstructure and processing. 2004; 375-377: 213-218.
[3] Zhang K, Fu Z, Effects of annealing treatment on phase composition and microstructure of CoCrFeNiTiAlx high-entropy alloys, Intermetallics. 2012; 22: 24-32.
[4] Hung P.K, Yeh J.W, S.T, Yeh J.W, Multi-Principal-Element Alloys with Improved Oxidation and Wear Resistance for Thermal Spray Coating. Advanced Engineering Materials 2004; 6: 74-78.
[5] JW Y, Recent progress in high-entropy alloys, European Journal of Control. 2006; 31: 633-648.
[6] MS C.T.S.I.Y.J.W, Nanostructured nitride films of multi-element high-entropy alloys by reactive DC sputtering, Surface and Coatings Technology. 2004; 188-189: 193-200.
[7] Chin You Hsu J.W.Y, Swe Kai Chen, Tao Tsung Shun, Wear resistance and high-temperature compression strength of Fcc $CuCoNiCrAl_{0.5}Fe$ alloy with boron addition, Metall Mater Trans A. 2004; 35: 1465-1469.
[8] Zhou Y.J, Zhang Y, Wang Y.L, Chen G.L, Solid solution alloys of AlCoCrFeNiTix with excellent room-temperature mechanical properties, Applied Physics Letters. 2007; 90.
[9] Li B.a, YP W, and Ren M.X and Yang C and Fu H.Z, Effects of Mn, Ti and V on the microstructure and properties of AlCrFeCoNiCu high entropy alloy, Mater Sci Eng A. 2008; 498: 498-482.
[10] Tong, C. J, Chen, M. R, Yeh J.W, Lin S.J, Lee P.H, Shun, T.T, et al. Mechanical performance of the AlXCoCrCuFeNi high-entropy alloy system with multiprincipal elements, Metallurgical and Materials Transactions A-physical Metallurgy and Materials Science - METALL MATER TRANS A. 2005; 36: 1263-1271.
[11] Xu Z, Li Z, Tong Y, Zhang W, Wu Z, Microstructural and mechanical behavior of a CoCrFeNiCu4 non-equiatomic high entropy alloy, Journal of Materials Science & Technology 2020; 60.
[12] Ren B.a, ZX L and Li, DM and Shi, L and Cai, B and Wang M.X, Effect of elemental interaction on microstructure of CuCrFeNiMn high entropy alloy system, Journal of Alloys and Compounds. 2010; 493: 148-153.
[13] Cantor B, Chang I. T. H, Knight P, Vincent a.A.J.B, Microstructural development in equiatomic multicomponent alloys. Materials Science and Engineering: A. 2003; 375–377: 213–218.
[14] Xiao L. L, Zheng Z. Q, Guo S.W, Huang P, and Wang F, Ultra-strong nanostructured CrMnFeCoNi high entropy alloys, Mater Des. 2020; 194: 108.
[15] Zhang F, Polymorphism in a high-entropy alloy, Nat Commun 8 (217).
[16] Lutterotti L, Maud: A Rietveld Analysis Program Designed for the Internet and Experiment Integration. Acta Crystallographica Section A - ACTA CRYSTALLOGR A. 2000; 56.
[17] Gonçalves A.P, Almeida M, Extended Miedema model: Predicting the formation enthalpies of intermetallic phases with more than two elements. Physica B: Condensed Matter. 1996; 228(3): 289-94.
[18] Takeuchi A, Inoue A, Classification of Bulk Metallic Glasses by Atomic Size Difference, Heat of Mixing and Period of Constituent Elements and Its Application to Characterization of the Main Alloying Element. Materials Transactions - MATER TRANS. 2005; 46: 2817-29.
[19] Uranaka S, Hirashima I, Maeda T, Masumura T, Tsuchiyama T, Kawamoto Y, et al. Quantitative Analysis of Hardening Due to Carbon in Solid Solution in Martensitic Steels. ISIJ International. 2023; 63(3): 569-78.